Journal of Advanced Research 23 (2020) 83–94

Contents lists available at ScienceDirect

Journal of Advanced Research

journal homepage: www.elsevier.com/locate/jare

New intranasal cross-linked mosapride xyloglucan pluronics micelles (MOS-XPMs) for reflux esophagitis disease: *In-vitro* optimization and improved therapeutic efficacy

Reham Waheed Hammad [a], Rania Abdel-Basset Sanad [a], Nevine Shawky Abdelmalak [b,c], Faisal A. Torad [d], Randa Latif [b,*]

[a] Department of Pharmaceutics, National Organization for Drug Control and Research, Giza, Egypt
[b] Department of Pharmaceutics and Industrial Pharmacy, Faculty of Pharmacy, Cairo University, Cairo, Egypt
[c] Department of Pharmaceutics, School of Pharmacy, New Giza University, NGU, Giza, Egypt
[d] Department of Surgery, Anesthesiology and Radiology, Faculty of Veterinary Medicine, Cairo University, Egypt

HIGHLIGHTS

- Mosapride was loaded inside crosslinked Xyloglucan Pluronic micelle (MOS-XPMs).
- (MOS-XPMs) showed improved stability and mucoadhesiveness.
- MOS-XPMs systems showed a rapid release of drug located in the shell within 0.5hr followed by a consistent release pattern for the remaining 8hr.
- Trans-abdominal ultrasonography XPMs showed 1.5 fold increased in duodenal and cecal motility compared to MOS suspension.

GRAPHICAL ABSTRACT

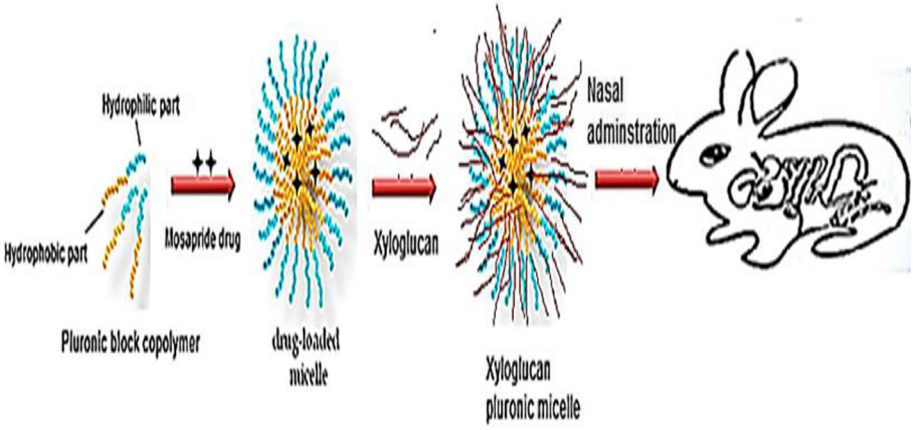

ARTICLE INFO

Article history:
Received 30 November 2019
Revised 24 January 2020
Accepted 25 January 2020
Available online 28 January 2020
New intranasal cross-linked mosapride xyloglucan pluronics micelles (MOS-XPMs) for reflux esophagitis disease

Keywords:
Mosapride citrate
Xyloglucan Pluronic micelles
Intranasal administration
Gastrointestinal motility

ABSTRACT

Mosapride belongs to class IV in Biopharmaceutics Classification System and is used in the treatment of reflux esophagitis. It exhibits poor bioavailability due to limited permeability, solubility and extensive first-pass metabolism. In this study, intranasal mosapride-loaded cross-linked xyloglucan Pluronic micelles (MOS-XPMs) was formulated and optimized to improve the low solubility & bioavailability of MOS. The solid dispersion technique using 2^3 full factorial design was applied. (MOS-XPMs) (F4) had the highest desirability value (0.952) and, therefore, it was selected as an optimal system. Xyloglucan cross-linked in the shell of Pluronic micelles offered improved stability and mucoadhesiveness to MOS-XPMs. ^{1}H NMR spectra ensured the cross-linking of xyloglucan with Pluronic micelle shell and micelle stabilization. A Pharmacodynamic study revealed that MOS-XPMs showed 1.5-fold increase in duodenal and cecal motility compared to MOS suspension and 1.7-fold increase compared to the oral marketed product. The new MOS-XPMs were shown to be successful at improving the therapeutic efficacy of mosapride.

Peer review under responsibility of Cairo University.
* Corresponding author at: Department of Pharmaceutics & Industrial Pharmacy, Faculty of Pharmacy, Cairo University. Kasr El Eini Street, Egypt.
E-mail address: latifranda@yahoo.co.uk (R. Latif).

https://doi.org/10.1016/j.jare.2020.01.013
2090-1232/

Introduction

Mosapride citrate (MOS) is a promising gastrointestinal prokinetic agent that enhances gastric motility without any reported side effects on the cardiac or nervous systems. It selectively stimulates serotonin 5-HT4 receptors [1]. It treats numerous gastrointestinal complaints, especially reflux esophagitis, [2] by improving the amplitude of esophageal peristalsis and gastric emptying time. Thus, it decreases the events of acid reflux to the esophagus and prevents ulcers, hemorrhage, and esophageal adenocarcinoma that can be a medical emergency. The poor solubility and wettability of MOS in addition to its short half-life and intensive first-pass metabolism led to a decrease in its bioavailability to be 8–14% [3]. The current versions of commercially available oral tablet dosage formulations of MOS cannot achieve the required therapeutic efficacy. The nasal route could be effective to achieve a direct systemic delivery of MOS escaping the hepatic metabolism to initiate peristalsis due to abundant vascularization and permeability of the nasal mucosa [4]. MOS is an ideal drug candidate for intranasal application because of its suitability in patients with swallowing problems and its low-dose requirement [5]. However, MOS may suffer from poor permeation through nasal mucosa. Furthermore, the intranasal delivery was bothered by several drawbacks, such as the mucociliary clearance which lowered the drug retention time and the enzymatic degradation [6]. Pharmaceutical nanotechnology has arisen as a perfect strategy to overcome these drawbacks [4]. Polymeric micelles (PMs) have been verified to overcome difficulties in intranasal drug delivery [6]. PMs are a core-shell nanostructure, where the hydrophobic core solubilizes lipophilic drugs and the hydrophilic shell stabilizes PMs in aqueous dispersion [6]. The inclusion of hydrophobic drugs into PMs is reported to improve their bioavailability through an increase in water solubility and wettability. PMs could guard the trapped drugs against nasal enzymatic degradation, and boost permeation across the nasal mucosa [4]. However, the lack of stability and dissociation upon dilution in biological fluids limited the use of PMs in drug delivery. Kabanov et al. introduced mixing hydrophobic and hydrophilic Pluronic copolymers [7] to stabilized prepared micelles. Recently, cross-linking the micellar shell has been a novel strategy introduced to ensure micellar stabilization and increased permeability. Lin stabilized and increased the mucoadhesivity of Pluronic nanomicelles by the use of hydrophilic chitosan polymer which thickened the micelle shells [8]. One such class of mucoadhesive polymers are polysaccharides [9]. These have a great impact on increasing mechanical strength and stability of drug delivery systems. Xyloglucan (XG) is a hemicellulose natural polysaccharide, present in the primary cell wall of the seed kernel of *Tamarindus indica* [10]. XG is generally used as a stabilizing, thickening, gelling and mucoadhesive agent. Furthermore, Xyloglucan structure is "mucin-like", having optimal mucoadhesion properties that increase the mucoadhesion of Pluronic micelles with mucosal surfaces. Xyloglucan has a balanced hydrophobic and hydrophilic character, facilitating the encapsulation of hydrophobic molecules [11]. Thus, it can be potentially used in polymeric micelle formulations to improve drug permeation [12]. In this study, nanoformulations of mosapride-loaded cross-linked xyloglucan Pluronic micelles (MOS-XPMs) were developed for intranasal administration. The novelty of this study is the cross-linking of xyloglucan in the shell of Pluronic micelles to augment contact time with the nasal mucosa and boost MOS permeation. To our knowledge, xyloglucan has neither been previously used as a nano-carrier in nasal formulations, nor used as a cross-linking polymer in the formulation of Pluronic micelles. Accordingly, the factors affecting the MOS-XPMs formulation intended to be applied intranasally will be studied as well as the effect of xyloglucan on the stabilization and mucoadhesion of the prepared MOS-XPMs.

Materials and methods

Materials

Western Pharmaceuticals, Obour city, Egypt, kindly gifted MOS. Pluronic P123 was procured from Sigma-Aldrich (St. Louis, MO, USA). Pluronic F127 was obtained from Sigma Aldrich, GmbH, Germany. Saiguru Food Gum Manufacturer Pvt. Ltd. (Mumbai, Maharashtra, India) supplied xyloglucan (average molecular weight 52,350Dalton) from *Tamarindus indicia*. Analytical grade and HPLC grade reagents were used.

Methods

Screening of polymer type and concentration for polymeric micelle preparation:

Pluronic F127, F68, P123 (which consist of polyethylene oxide (PEO) and propylene oxide (PPO) blocks) and xyloglucan were used. Screening of the most suitable polymer type and concentration was performed according to phase solubility technique established by Higuchi [13]. Different weight ratios of MOS to copolymers were added in aqueous solutions (1/2, 1/5, and 1/8) and shaken at 37 °C for 48hrs. The increase in MOS aqueous solubility was assayed spectrophotometrically at 308 nm [4]. The Gibbs free energy of transfer (ΔGtr°) of MOS from water to aqueous solutions of polymers was calculated using Eq. (1) [14].

$$\Delta G_{tr}\hat{A}^{o} = -2.303RT\log\left(\frac{Sc}{So}\right) \quad (1)$$

where R (8.314 J $mol^{-1}K^{-1}$) is the universal gas constant, T is temperature (310° Kelvin) at which the phase solubility study was conducted, and Sc/So is the ratio of molar solubility of MOS in the aqueous solution of polymers to that of water. Obtained values of ΔGtr° indicate whether the drug solubilization in the aqueous solution is favorable or not (negative $\Delta G_{tr^{\circ}}$ values indicate favorable conditions).

Preparation of mosapride-loaded xyloglucan Pluronic micelles (MOS-XPMs)

The MOS-XPMs was prepared using a solid dispersion technique [15,16]. MOS and Pluronic copolymers were dissolved in 4 ml of ethanol (Table 1). After 30 min of stirring, ethanol was evaporated under reduced pressure at 60 °C and a thin dry film was formed on the inner wall of the flask. The film was hydrated with different concentrations of xyloglucan solution (dissolved in distilled water

Table 1
The experimental plan of the factorial design 2^3 for the preparation of mosapride Pluronic micelle formulations for intranasal delivery.

Independent Variables	Level	
	−1	1
A* = Pluronic P123: P127 Ratio	70:30	30:70
B* = Drug: Pluronic Ratio	1: 2	1:5
C = Xyloglucan Concentration (w/v %)*	0.5%	1%
Dependent Variables	**Constraints**	
Y_1 = Particle Size	Minimize	
Y_2 = Percentage of Entrapment Efficiency (%EE)	Maximize	
Y_3 = Percentage of Drug Loading (% DL)	Maximize	
Y_4 = Percentage Release after 0.5hr	Maximize	
Y_5 = Percentage Release after 8hr	Maximize	

*Drug concentration is kept constant to be 5 mg/ml while Pluronic concentration used was 10 mg/ml for drug: Pluronic ratio (1:2) and 25 mg/ml for drug Pluronic ratio (1:5).
*The Pluronic F127 concentration was 30% of the Pluronic P123: P127 ratio(70:30) and 70% of the Pluronic P123: P127 ratio(30:70).

by gentle heating to 50–60 °C with continuous stirring for 3hr [17], at 60 °C using magnetic stirring (210 rpm) for 1 h under normal pressure [8]. Finally, the resultant xyloglucan polymeric micelle dispersion (MOS-XPMs) was filtered through a 0.45 μm filter. Table 2.

Optimization by factorial statistical design

A 2^3 full-factorial design was used to define the optimum factors to develop MOS-XPMs. Dependent and independent variables and desirability constraints are demonstrated in (Table 1). Various *MOS-XPMs* systems were prepared by using all possible combinations of different levels of experimental variables. The statistical analysis of responses was done by Design-Expert® Software (Stat-Ease Inc., Minneapolis, MN, USA).

Characterization of the prepared MOS-XPMs

Determination of particle size, entrapment efficiency and drug loading of MOS-XPMs

The mean particle size and polydispersity index of the prepared MOS-XPMs were determined by photon correlation spectroscopy (Malvern Instruments, Zetasizer 3000, UK).

The entrapment efficiency percentage (EE %) and drug loading percentage (%DL) were calculated according to the method described by Nour et al. [6]]. 1 ml of the separated MOS-XPMs was disrupted by sonication with ethanol (selected as an appropriate solvent for the lyses of the prepared MOS-XPMs). The concentration of the entrapped drug was measured spectrophotometrically at 308 nm. The %EE and %DL were calculated using equations (2, 3).

$$\mathbf{EE}\% = \frac{\mathbf{Amount\ MOS\ entrapped\ (mg)}}{\mathbf{total\ Amount\ MOS\ (mg)}} \times 100 \quad (2)$$

$$\mathbf{DL}\% = \frac{\mathbf{Amount\ MOS\ entrapped(mg)}}{\mathbf{total\ Amount\ MOS(mg) + A}\boldsymbol{mount\ of\ polymer} \times 100 \quad (3)$$

In-vitro drug release

A dialysis method was used to investigate the *in-vitro* release of MOS from different MOS-XPMs [4]. 1 ml of the filtered MOS-XPMs dispersion (according to the predetermined %EE), was placed in a dialysis bag (molecular weight cut-off: 12,000–14,000 Serva Electrophoresis, Germany). Bags were sealed and immersed in USP dissolution apparatus type II (Agilent, USA) containing 50 ml of 30% (v/v) ethanolic phosphate buffer saline pH 6.0, stirred at 100 rpm at 37 ± 0.5 °C. Samples were withdrawn at time intervals (0.25, 0.5, 1, 2, 4, 6, 8hr) and the percentage of MOS released was quantified spectrophotometrically at 308 nm. A statistical analysis was done for the percent of MOS from MOS-XPMs after 0.5hr ($Q_{0.5hr}$) and 8hr (Q_{8hr}). *In-vitro* drug release data were fitted to various kinetic models [4] (zero order, first order, Higuchi model, Korsmeyer-Peppas model, in addition to Weibull model, and regression analysis was performed to investigate the mechanism of MOS release from MOS-XPMs).

Selection of the optimized formulation

Design Expert software supported the selection of optimized MOS-XPMs with constraints of desirability presented in Table (1). Validation of the design of MOS-XPMs was done by ANOVA provision available in the software [4].

Transmission electron microscopy (TEM)

The morphology of the optimized MOS-XPMs system was examined by a TEM (Jeol JEM 2100, Japan). The sample was located onto a copper grid coated with collodion film. Then a process of negative staining to the sample was executed by the aid of phosphotungestic acid. Finally, drying at room temperature was done before TEM examination [6]].

Differential scanning calorimetry (DSC) and fourier transform infrared spectroscopy (FT-IR)

Optimized MOS-XPMs, components (xyloglucan and PF127) and pure MOS were examined by DSC (Q A20, Germany) at a rate of 10 °C/min in a nitrogen atmosphere in a range of 25°–200 °C [4]. Additionally, they were examined by *FT-IR* (Cary 620, USA) at a wave number ranging from 400 to 4,000 cm^{-1}.

Nuclear magnetic resonance (NMR)

The cross-linking characteristics in the shell of the optimized MOS-XPMs system were investigated using ^1H NMR spectra on Bruker-ARX 400, Germany. PF127, Xyloglucan and MOS solutions were prepared by mixing with double distilled water and stirred for approximately 3hr until complete dissolution [18]. All samples were dissolved in deuterated water (D_2O) for NMR measurements at room temperature.

Zeta potential determination, in-vitro mucoadhesion and physical stability assessment

The Zeta potential of the optimized MOS-XPMs was investigated using Malvern Instruments (Zetasizer 3000, UK) [6].

In-vitro mucoadhesion was investigated through a modified falling liquid film technique to ensure the mucoadhesion property of the optimum MOS-XPMs formulation [17]. A fresh piece of sheep nasal mucosa (excised within 1hr of sacrificing the animal), was washed with isotonic saline solution and held horizontally over a glass plate. 0.5 ml of the filtered MOS-XPMs dispersion (according to the predetermined %EE) was located on the mucosal surface. After a period of 30 min, it was tilted at an angle of 45° to allow for the drainage of the non-adhered drug. MOS concentration was determined spectrophotometrically at 308 nm. The percentage mucoadhesion was determined using Eq. (4).

$$\%\mathbf{Mucoadhesion} = \frac{\mathbf{A - B}}{\mathbf{A}} \times 100 \quad (4)$$

Where A is the actual MOS amount in MOS-XPMs; B MOS amount in the collected perfusate.

Table 2
Phase solubility study of MOS in distilled water in presence of different polymers concentrations ± S.D, and thermodynamic parameters of the solubility process of MOS in water-polymers system.

	F127		P123		F68		Xyloglucan	
	Amount dissolved (μg/ml)	$\Delta G_{tr}°$ (KJ/mol)	Amount dissolved (μg/ml)	$\Delta G_{tr}°$ (KJ/mol)	Amount dissolved (μg/ml)	$\Delta G_{tr}°$ (KJ/mol)	Amount dissolved (μg/ml)	$\Delta G_{tr}°$ (KJ/mol)
1:2	1592.49 ± 71.68	−9245.5	1438.49 ± 67.66	−8983.4	1562.62 ± 72.19	−9196.73	1488.86 ± 70.93	−9072.08
1:5	1738.84 ± 81.32	−9472.2	2134.80 ± 113.99	−10001.02	1543.36 ± 73.46	−9164.75	1319.09 ± 63.23	−8759.99
1:8	1649.38 ± 83.07	−9336.02	1787.56 ± 92.12	−9543.4	1570.01 ± 73.87	−9208.89	1485.44 ± 79.24	−9066.15

• Saturated solubility of MOS in distilled water was found to be 44.1 ± 0.03 μg/ml.

For the physical stability assessment, the optimized MOS-XPMs system was stored at room temperature over 24hr. The transmittance (T%) was investigated spectrophotometrically (λ_{max}520nm) using de-ionized water as a blank [19]. The turbidity of MOS-loaded micelles was calculated according to equation (5):

$$\textbf{Turbidity} = \frac{(100 - \%\mathbf{T})}{100} \quad (5)$$

In-vitro permeation study

Mosapride suspension and the optimum MOS-XPMs were tested for permeation according to the method described by Hammad et al [4]. Both, the suspension and the MOS-XPMs formula were exposed to the surface of sheep nasal mucosa, rotated at 50 rpm in100mL of phosphate buffer pH 6.0 kept at 37 ± 0.5 °C. Samples were taken at specific time intervals. The amount of permeated drug was assayed spectrophotometrically at 308 nm. All parameters concerning permeation data were subsequently calculated [4].

Pharmacodynamic study in rabbits

Animals

The Institutional Ethical Committee (Faculty of Pharmacy, Cairo University) (S.No.PI1081) revised and approved the animal study protocol. The design and details of experiments were carried out following the methods previously described by Hammad et al [4]. In brief, a cross-over design was applied to fifteen rabbits with a wash-out period of one week. After intranasal delivery of the respective doses, the duodenal and cecal motility were investigated by *trans*-abdominal ultrasonography using 10 MHz micro-convex transducer (Esoate Digital) with color doppler ultrasound system (Mylabone Co., Ltd.).

Statistical analysis was executed using a statistical software program (SPSS Inc., Chicago, USA). The statistical difference between groups and control was determined by one-way ANOVA (at 95% confidence limit (α = 0.05)) [4].

Nasal histopathology

In order to exclude the possibility of any toxic effect concerning the intranasal administration of the prepared nanomicelles, a histopathological examination was executed following the methods described by Hammad et al. and Shah et al. [420]. Three sectors of sheep nasal mucosa were selected and treated with negative control (phosphate buffered saline pH 6.4), positive control (isopropyl alcohol), and MOS-XPMs, respectively, for 1hr. Afterwards, the mucosa was examined under optical microscope (Olympus CX31, Japan) to elucidate any variation that might occur to different tissues of nasal mucosa.

Results and discussion

Screening of polymer type and concentration for polymeric micelle preparations

MOS is practically insoluble in water with aqueous solubility 44.1 ± 0.03 μg/mL. The solubility of MOS increased in different polymer solutions, which could probably be attributed to the increased wettability of MOS and micellar solubilization [14]. Table (2) presents the thermodynamic parameters obtained with the aqueous solubility of MOS in the presence of Pluronic (F127, P123, F68) and xyloglucan. MOS solubility increased in the presence of all tested polymers. ΔGtr° values were all negative, indicating the spontaneous solubilization of the drug which decreased as polymer concentrations increased, [14] demonstrating that the reaction became more favorable as the concentration of polymers increased from 1:2 to 1:5. Higher concentration of these polymers (1:8) led to a decrement of drug solubility due to the increased viscosity of the diffusion boundary layer adjacent to the dissolving surface [21]. MOS showed the highest solubility in Pluronic P123 (PP123) ($EO_{20}PO_{69}EO_{20}$) with (HLB value = 8) and Pluronic F127 (PF127) ($EO_{99}PO_{65}EO_{99}$) (with HLB value = 22). Therefore, further studies were limited to these two Pluronic types. The ratio of MOS to Pluronic was maintained at a maximum of 1:5 w/w.

Preparation of MOS-XPMs

Solid dispersion method involves evaporation of ethanol yielding a melted Pluronic film where Pluronic–drug interactions are favored. Rehydration with a heated aqueous solution containing xyloglucan produces drug-loaded micelles. PF127 and PP123 with similar PPO moieties showed cooperative aggregation that the inner core related to hydrophobic PPO blocks and the outer shell to the hydrophilic PEO blocks. Xyloglucan cross-linked and thickened the hydrophilic shell.

Statistical analysis of data and validation of the optimization model

2^3 full-factorial design was used to define the optimum factors to develop MOS-XPMs. The effect of Pluronic ratio PP123: PF127 (A), the drug Pluronic ratio (B), and the concentration of xyloglucan (C) on the dependent variables of the prepared MOS-XPMs shown in Table 1 was assessed using Design-Expert® software (version 7; Stat-Ease, Inc., Minneapolis, MN, USA). Polynomial equations of different dependent variables are shown below in the terms of coded factors:

$$Y_1 = +91.98 - 7.65A + 7.39B + 2.98C + 5.34AB - 2.58AC + 4.46BC + 2.89ABC \quad (6)$$

$$Y_2 = +64.21 + 9.94A - 4.98B + 1.17C + 2.77AB - 0.40AC - 4.42BC + 1.48ABC \quad (7)$$

$$\boldsymbol{Y}_3 = +16.72 + 2.01A - 6.84B + 0.41C + 0.11AB + 0.025AC - 0.95BC + 0.15ABC \quad (8)$$

$$\mathbf{Y}_4 = +28.63 - 3.89A - 0.61B + 5.28C - 0.92AB + 3.44AC + 0.48BC - 0.65ABC \quad (9)$$

$$Y_5 = +53.27 - 6.78A + 1.06B + 10.91C + 0.17AB + 5.38AC + 3.42BC + 0.091ABC \quad (10)$$

The adequate precision for particle size was 34.426 with reasonable difference between the predicted r^2 (0.9648) and the adjusted r^2 (0.9835). The adequate precision for EE% was 24.448 with reasonable difference between the predicted r^2 (0.9317) and the adjusted r^2 (0.9680). Regarding DL%, the adequate precision was 36.75 with reasonable difference between the predicted r^2 of (0.9781) and the adjusted r^2 (0.9897). The adequate precision for release after 0.5hr was 35.55 with reasonable difference between the predicted r^2 (0.9755) and the adjusted r^2 (0.9885). The adequate precision for release after 8hr was 36.321 with reasonable difference between the predicted r^2 (0.9737) and the adjusted r^2 (0.9877).Therefore, the adequate precision of dependent variables were indicating a good correlation between the independent variables and the validity of the optimization model.

Characterization and evaluation of the prepared MOS-XPMs

Particle size determination (Y_1)

All systems were found (Table 3) in a nano-size range of 64.65 ± 1.77 nm to 108.31 ± 1.37 nm with adequate values of the polydispersity index (PDI) of 0.14 ± 0.01 to 0.28 ± 0.05 (Table 3). Statistical analysis showed that all three variables and their interaction significantly affected the mean particle size ($p < 0.05$) (Fig. 1).

MOS-XPMs with PP123:PF127 ratio **(A)** of 70:30 had significantly larger particle sizes than those prepared at the ratio 30:70. According to Hussein and Youssry [22], the increase in the hydrophobic core size correspondingly increased the aggregation number of micelles which consequently led to the formation of lamellar aggregates with larger sizes [23]. The highest positive coefficient of drug-to-Pluronic ratio (B) shown in equation (6) confirmed its effectiveness on the particle size. The increase in the drug-to-Pluronic ratio to 1:5 could result in the increase in the particle size due to increased aggregation number. Vorobyova et al. [24] and Amann et al. [25] discussed the increased aggregation number with increased polymer concentrations. Increasing xyloglucan concentration (C) resulted in a significant increase in the particle size of the prepared MOS-XPMs. This could be attributed to the hydrogen bonding between the ether oxygen of PEO chains in the P123/F127 binary mixture and the hydroxyl group (OH) of xyloglucan, which might have enriched the micelle shell [26].

Determination of the entrapment efficiency (%EE) (Y_2) and drug loading (%DL) percentages of the prepared MOS-XPMs (Y_3)

The results in Table 3 show that %EE ranged from 42.19 ± 1.47% to 80.07 ± 2.42%. The %DL ranged from 7.03 ± 0.24% and 26.69 ± 0.81%. The highest positive coefficient of PP123: PF127 ratio (A) (in Eqs. (7) and (8) confirmed its significant influence on the %EE and %DL ($P < 0.05$). It was previously reported that the critical micelle concentration (CMC) values of PP123 and PF127 were 0.0068% and 0.0021%, respectively, and the CMC of PP123/PF127 binary mixture was determined to be 0.0059% [27]. The lower CMC for PF127 (PPO length: 65) and PP123/PF127 mixture compared to PP123 (PPO length: 69) were elucidated. The CMC of PMs systems containing PP123:PF127 ratio of 30:70 could be lower compared with those containing the 70:30 ratio. Thus the decrease in CMC in system with PP123:PF127 ratio of 30:70 could lead to the formation of more micelles and consequently increase the % EE and %DL [28]. This result agreed with Mingkwan et al. [29] who concluded that the lower CMC of P123/TPGS mixed micelles resulted in increasing the %EE and %DL. Furthermore, PF127 has a higher molecular weight (MW) than P123. According to Raval et al., the Pluronic with higher MW has higher %EE and %DL [30]. The high negative coefficient of drug-to-Pluronic ratio (B) in equations (7, 8) confirmed that the MOS-XPMs systems containing drug-to-Pluronic ratio of 1:2 increased in %EE and %DL compared with systems with a weight ratio of 1:5 which contained a higher PEO/PPO ratio. As higher PEO/PPO ratio might reduce the hydrophobicity of the core [31], the quantity of the drug entrapped in micelle decreased with the higher Pluronic contribution of 1:5 (Fig. 1). Statistical analysis also revealed that xyloglucan concentration (C) had a significant effect on %DL ($p < 0.1$) of the prepared MOS-XPMs. This could be explained on the basis that xyloglucan contains a balanced hydrophobic and hydrophilic character, facilitating the encapsulation of the drug [11].

In-vitro release study of MOS from prepared (MOS-XPMs) systems

The *in-vitro* release profile of MOS from all MOS-XPMs systems showed a rapid release of the drug located in the shell or at the core-shell interface within 0.5hr (as shown in Fig. 2), followed by a slow-release pattern for the remaining 8hr. The slow-release pattern resulted from the low CMC of the prepared Pluronic micelles, which imparted thermodynamic stability to the prepared micelles, overcoming the sinking condition and drug retention in the micelles under considerable dilution [22]. The statistical analysis of %MOS released after 0.5hr and 8hr was investigated, concluding that all the three variables and their interaction significantly affected the mean percentage of MOS released ($p < 0.05$) (Fig. 1).

MOS-XPMs with PP123:PF127 ratio (A) of 30:70 showed a slower release profile of MOS than the 70:30 ratio (Fig. 2). This could be interpreted by the higher concentration of PF127, which could lower the CMC of the micelles. Furthermore, PF127 has higher molecular weight and higher PEO content (about 200) than PP123, which means more abundance of O and OH points that enhanced attachment via hydrogen bonds between the amine and amido groups of MOS and the ether oxygen and OH groups of PEO chains [26]. A stable bond led to a deep localization of MOS at the core-shell interface into the micellar interior and slower release of MOS. This also explained the lower release profile at high polymer concentration containing the drug-to-Pluronic ratio (B) of 1:5 **(**Fig. 2).

The highest positive coefficient of xyloglucan concentration (C) (in equations (9),10) confirmed its great effect on the % MOS released after 0.5 h and 8hr, respectively, from the prepared MOS-XPMs. The incorporation of the hydrophilic xyloglucan copolymer led to the formation of more hydrophilic channels, which enhanced the distribution of more water molecules into the core of micelles and, consequently, higher % MOS released [27]. The positive interaction coefficient (AC) in equations (9, 10) confirmed that cross-linking at the micellar shell, resulting from hydrogen bonding at ether oxygen of PEO chains of PF127 and the OH groups of xyloglucan, which, in turn, decreased hydrogen bonds between MOS and PF127, led to increased %MOS released after 0.5hr and 8hr, respectively.

Release kinetics of MOS from the prepared (MOS-XPMs)

The release of MOS from all systems followed the Weibull model (R^2 ranged from 0.911 to 0.98) which offers a simple physical connection between the drug release and system geometry

Table 3
The mean particle size, polydispersity index, the percentage entrapment efficiency (%EE) and the percentage drug loading (%DL) of MOS in the prepared MOS-XPMs formulations ± SD.

System Code	Mean particle Size (nm)	Polydispersity Index	Entrapment Efficiency (%)	Drug Loading (%)
F1	93.58 ± 1.66	0.14 ± 0.01	54.55 ± 2.07	20.17 ± 1.01
F2	101.58 ± 1.44	0.28 ± 0.05	69.49 ± 2.39	23.16 ± 0.80
F3	78.56 ± 2.33	0.22 ± 0.07	72.64 ± 3.77	24.21 ± 1.26
F4	64.65 ± 1.77	0.17 ± 0.07	80.07 ± 2.42	26.69 ± 0.81
F5	94.55 ± 1.85	0.22 ± 0.01	50.86 ± 1.92	8.48 ± 0.32
F6	108.31 ± 1.37	0.23 ± 0.02	42.19 ± 1.47	7.03 ± 0.24
F7	89.31 ± 1.76	0.20 ± 0.01	74.13 ± 3.43	12.36 ± 0.57
F8	104.81 ± 1.44	0.28 ± 0.01	69.76 ± 2.72	11.63 ± 0.45

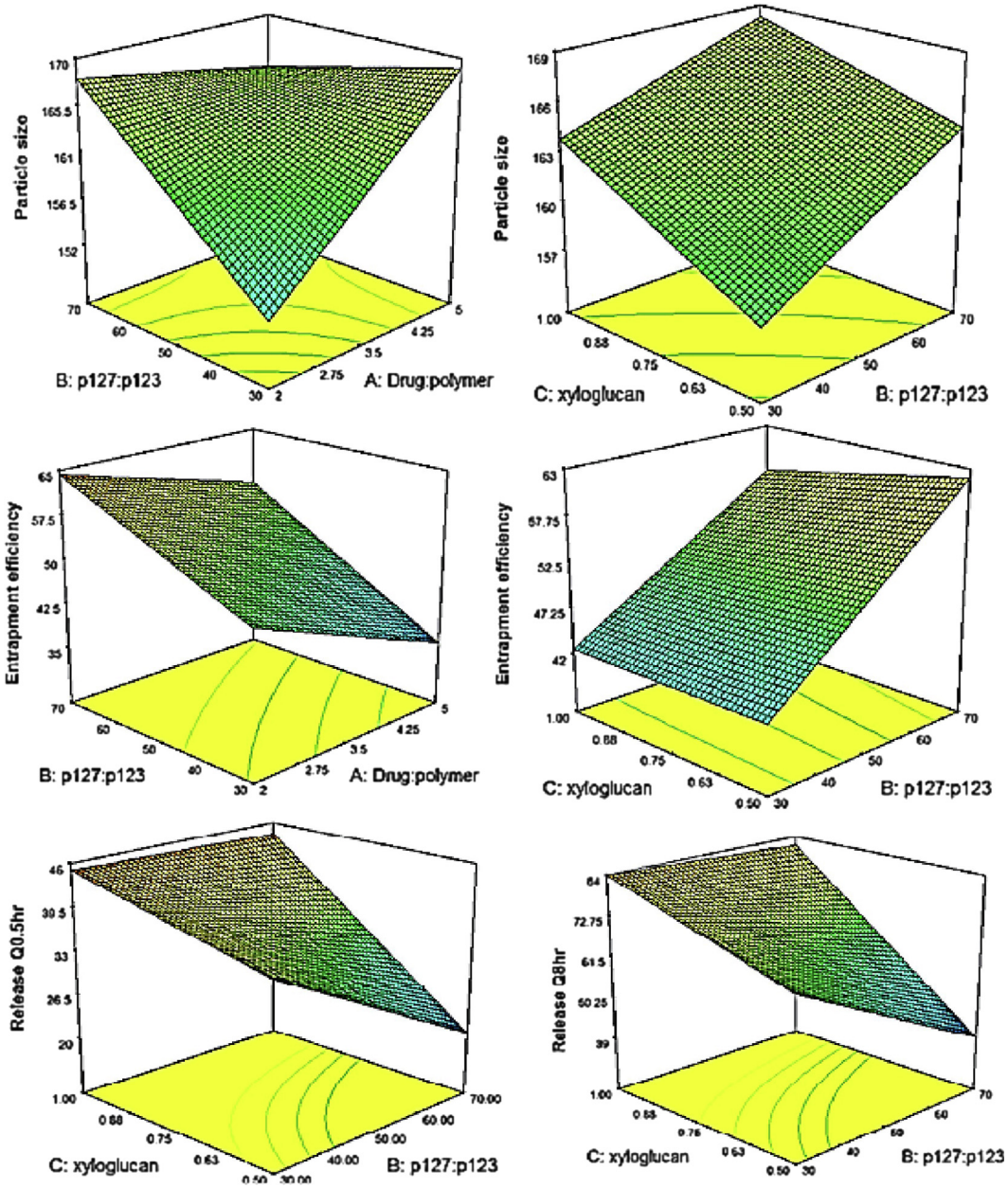

Fig. 1. 3D response surface plot of factor showing effect of xyloglucan concentration(C) versus Pluronic (PF127:PP123) (A) on the dependent variables (particle size, EE%, DL%, Q0.5hr and physical stability) of the prepared MOS-XPMs systems for drug: Pluronic ratio(1:2) (B).

[32]. The release behavior from the MOS-XPMs systems can be recognized from the value of the exponent (b) in the Weibell equation [33]. The values of b for all MOS-XPMs systems were in the range (0.39 < b < 0.69–0.75), which, according to Kosmidis et al. [33], reflected that the drug release from MOS-XPMs systems followed Fickian diffusion. For the Fickian diffusion, the micelles with the uptake of water would swell, especially in the presence of 1% of hydrophilic xyloglucan polymer, and allow the drug within to diffuse through the pores.

Optimization of the prepared (MOS-XPMs)

Based on the desirability criterion (Table 1), the system **MOS-XPMs (F4)** containing the Pluronic (PP123:PF127) ratio of 30:70, drug-to-Pluronic ratio of 1:2, and xyloglucan concentration (1% wt.) was found to fulfill the maximum requisite of an optimum formulation with maximum desirability (0.903).

Transmission electron microscopy (TEM)

The TEM micrographs of the optimized MOS-XPMs (F4) showed small-sized uniform spherical shaped micelles arranged in clusters (Fig. 3a). The outer dark shell attributed to the cross-linking of xyloglucan and Pluronics due to hydrogen bonding and inner bright core should relate to hydrophobic PPO. The mean particle size demonstrated by TEM (39.87 nm ± 6) was smaller than that measured by the Zetasizer (64.65 ± 1.77), and size differences were due to the effect of drying [10]].

Differential scanning calorimetry (DSC) and fourier transforms infrared spectroscopy (FT-IR)

DSC study of MOS and PF127 showed a sharp melting endothermic peak (Fig. 3b) at about 116 °C and 53.65 °C, respectively (corresponding to their melting points). Xyloglucan showed a sharp endothermic peak at about 57.65 °C and an exothermic peak at

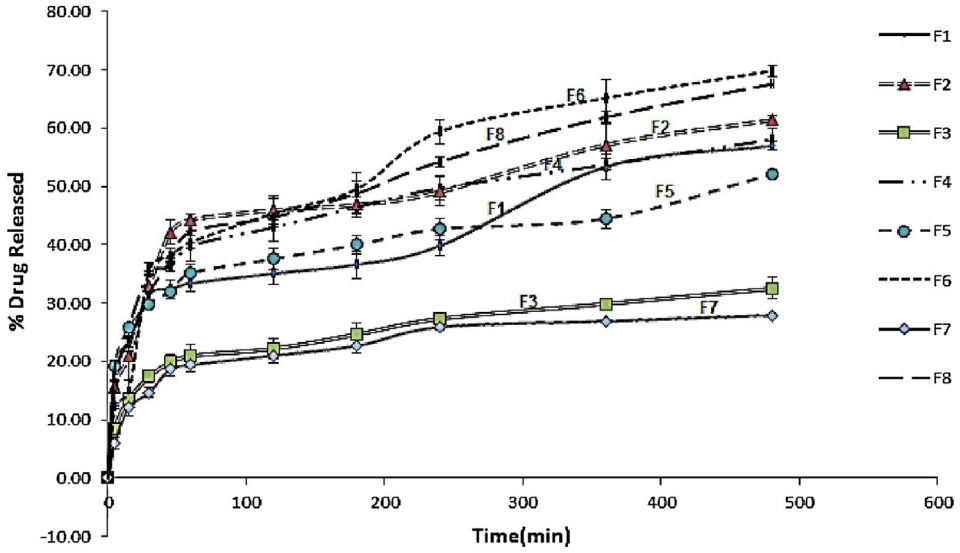

Fig. 2. Release pattern of MOS from MOS- XPMs systems ± SD.

78.86 °C. The thermogram of the optimized MOS-XPMs (F4) showed the presence of one sharp endothermic peak at 52.75 °C and an exothermic peak at 86 °C. A complete disappearance of the melting endotherm of MOS indicated homogenous dispersion of MOS in the developed MOS-XPMs. The enthalpy of the endothermic peak corresponding to xyloglucan, Pluronic F127, and MOS-XPMs (F4) formulation were measured at 25 J/g, 19.8 J/g, and 28.21 J/g, respectively. An exothermic crystallization enthalpy value corresponding to xyloglucan and MOS-XPMs (F4) formulation were investigated at 34.14 J/g and 46 J/g, respectively, during cooling scans. The significant increase in endothermic and exothermic enthalpy might be due to the micellization and crystallization of MOS-XPMs blocks induced by higher concentration of hydrophobic MOS encapsulated within the micelle cores [34,35].

By studying the FT IR spectrum of MOS-XPMs (F4) and comparing it with Pluronic and xyloglucan spectrum (Fig. 3c), MOS-XPMs (F4) showed complete disappearance of characteristic absorption bands of MOS and Pluronic, and showed one characteristic absorption band at 1658 cm^{-1} corresponding to the bending vibrations of –OH of xyloglucan, but with decreased intensity. This might be due to the hydrogen bonding effects between the ether oxygen of PEO chains in PP123/PF127 and the hydroxyl group of xyloglucan which enriched micelle shells.

Nuclear magnetic resonance (NMR)

Nuclear magnetic resonance (NMR) is a precise method to investigate the chemical structures [18]. It was used to ensure the cross-linking between the block copolymer PF127 and xyloglucan. Fig. 3d shows ^{1}H NMR spectra obtained from the prepared MOS-XPMs, PF127, xyloglucan and MOS solutions. The ^{1}H NMR spectra for MOS-XPMs revealed the disappearance of MOS characteristic peaks, while the peaks related to PF127 and xyloglucan were still identified. These findings ensured successful solubilization and stabilization of MOS within the hydrophobic core. Xyloglucan showed a weak singlet peak at 2.13 corresponding to the signal of a hemiacetal group (HO-C-O-C). The multiple peaks between 2.6 and 2.8 ppm in MOS-XPMS (F4) spectrum indicated the excessive hydrogen bonding between OH groups of xyloglucan and ether oxygen of PF127. This hydrogen bond has been detected to result in splitting and increase in the chemical shift of the coupled protons in the neighboring hydrogen bond [36].

Zeta-potential determination, in-vitro mucoadhesion and physical stability assessment

The zeta-potential of the optimized MOS-XPMs (F4) was measured to be −17.1 mV ± 0.071. The structure of P123 and F127 was non-ionic [26]. The negative charge resulted from the presence of anionic xyloglucan in the shell of mixed micelles which could stabilize the prepared MOS-XPMs and minimize micelle aggregation.

MOS-XPMs (F4) showed a percentage mucoadhesion to be 68.69% ±2.00 after 0.5hr due to the presence of mucoadhesive xyloglucan which could prolong the contact time, counteract the mucociliary clearance, and improve drug permeation through nasal mucosa [37]. Xyloglucan has a good mucoadhesive property as due to its cellulose-like backbone chain with mucin-like configuration. The secondary hydroxyl (OH) groups that exist in xyloglucan are the principal source of mucoadhesion and confer anionic charge.

The physical stability of the optimized MOS-XPMs system was determined by measuring the transmittance percentage (%T). Low transmittance percentage and the presence of turbidity in the system are usually attributed to the transient separation of large micelles and/or drug molecules [38]. MOS-XPMs (F4) showed a low percent of turbidity (% T = 82.11%) [19] due to its higher solubilizing capacity for poorly water-soluble MOS and provides higher stability [38] which led to an increase in the amount of drug entrapped in polymeric micelle. The PP123 and PF127 have similar number of PPO units, which would allow the development of very stable micelles [19]. The presence of PP123:PF127 ratio with a different hydrophilic-lipophilic balance (HLB) could result in thermodynamic and kinetic stability for the prepared MOS-XPMs. Low HLB of PP123 would increase the thermodynamic stability of MOS-XPMs micelles due to the tight hydrophobic interactions. On the other hand, the cross-linking of PF127 together with xyloglucan in Pluronics shell would increase the kinetic stability of MOS-XPMs due to the anionic charge that minimizes micelle aggregation [39] and maximizes micelle stability; thus, lowers turbidity.

In-vitro permeation study

The results of *in-vitro* permeation are shown in Table 4. Results revealed that a threefold increase in permeation of MOS occurred from MOS-XPMs (F4) (92.5% ±2.17) with respect to MOS

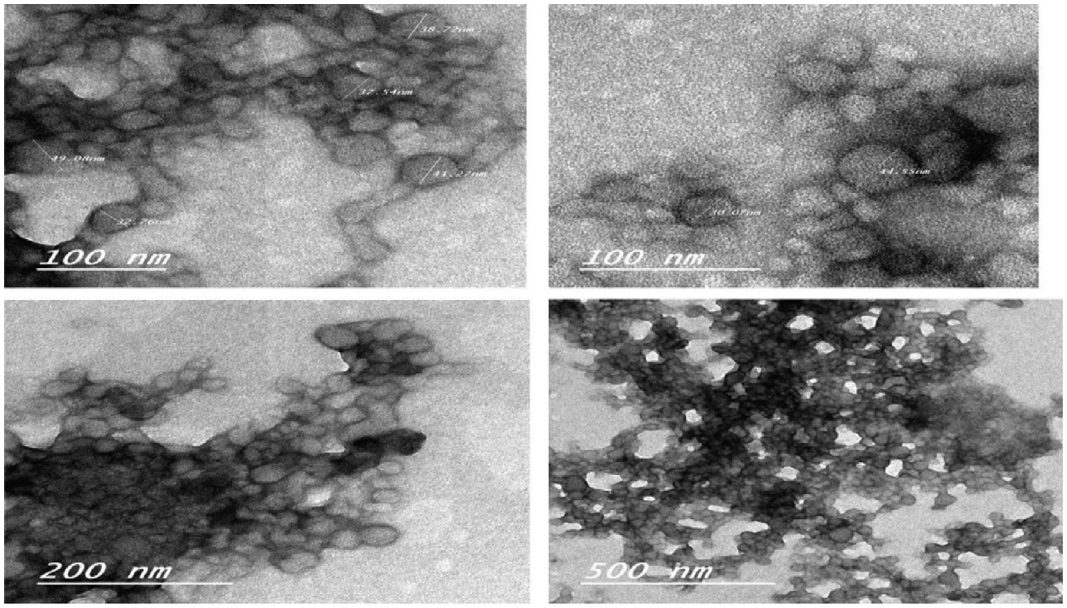

a

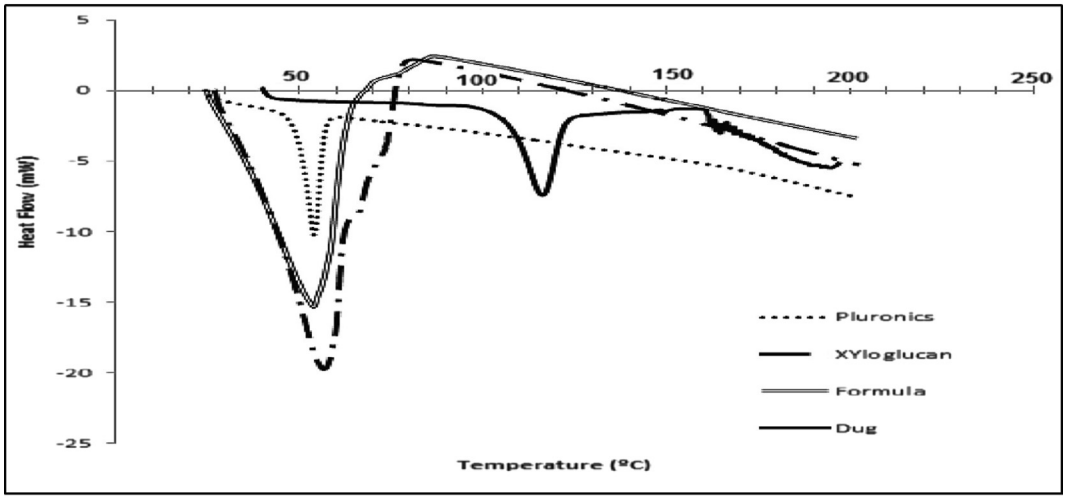

b

Fig. 3. (a) TEM image of the optimized MOS-XPMs(F4). (b) DSC curve of pure drug, components (xyloglucan and Pluronic F127) and MOS- XPMs (F4). (c) FTIR curves of MOS-XPMs(F4), xyloglucan, Pluronic F127 and drug. (d) NMR spectra of MOS-XPMs(F4), xyloglucan, Pluronic F127 and drug.

suspension (31.77% ±0.1). The low permeability and ionization of MOS at the pH of the nasal epithelium bothered its intranasal delivery. The optimized MOS-XPMs (F4) improved nasal permeation through the mucoadhesion properties of xyloglucan, which enhanced the contact with the nasal mucosa and decreased mucociliary clearance [37]. Furthermore, XPMs with small size and improved water solubility of MOS could result in rapid hydration and permit permeation through paracellular route [40].

Pharmacodynamic study in rabbits:

The use of anaesthetizing agents was avoided to maintain the functional mucociliary clearance, so that the *in vivo* absorption of MOS was not affected [4].

The duodenal and cecal contractions were quantitatively studied (Fig. 4 a, b) and assessed from 15 min to 180 min after MOS administration. The average contractions before MOS administration (control) were assessed to be 8.84 ± 0.61 contractions/min. After the administration of MOS, the rate of contraction at T_{max} changed to 15.18 ± 1.6 contractions/min for MOS-XPMs, 10.02 ± 0.62 contractions/min for MOS suspension, and 8.9 ± 0.72 contractions/min for commercial MOS oral tablets. Doppler ultrasonography showed that MOS-XPMs not only increased the average contractions per minute but also increased their intensity (as shown in Fig. 4b). One-way ANOVA showed that commercial MOS oral tablets had no significant increase in the duodenal and cecal contractions ($P > 0.05$) after oral MOS administration owing to their low oral bioavailability. However, intranasal MOS-XPMs had a significant increase in the duodenal and cecal contractions than MOS suspension, which was attributed to a higher permeation rate of the prepared MOS-XPMs. These results were consistent with the results *of in-vitro* permeation; therefore, the inclusion of MOS into intranasal MOS-XPMs achieved the goal of the study and improved the clinical efficacy of MOS.

Nasal histopathology

Negative control-treated mucosa appeared intact with a preserved structure. After treating mucosa with MOS-XPMs, neither cell necrosis nor structural damage was detected (Fig. 5). Positive

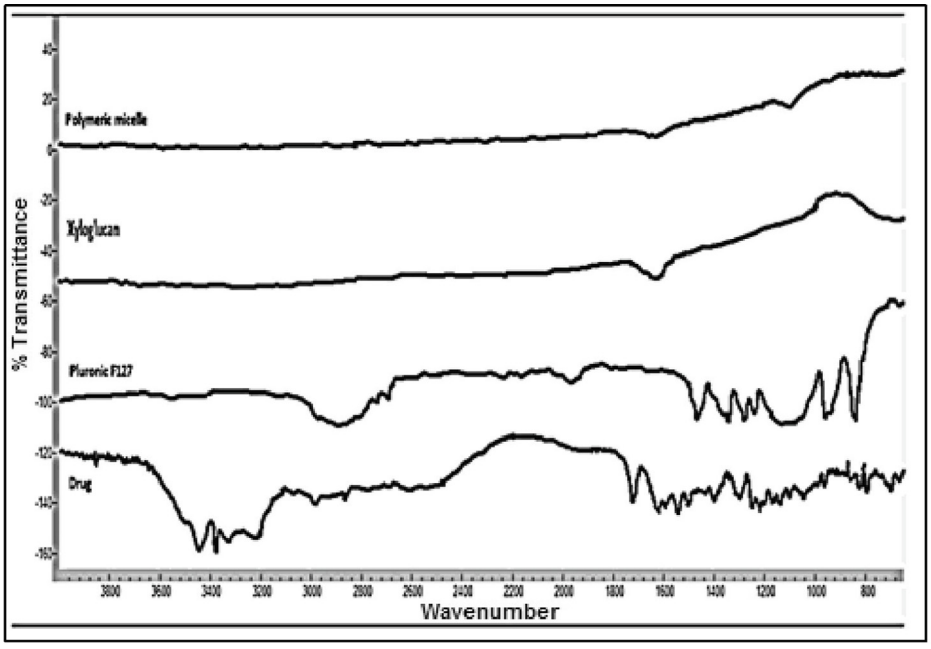

c

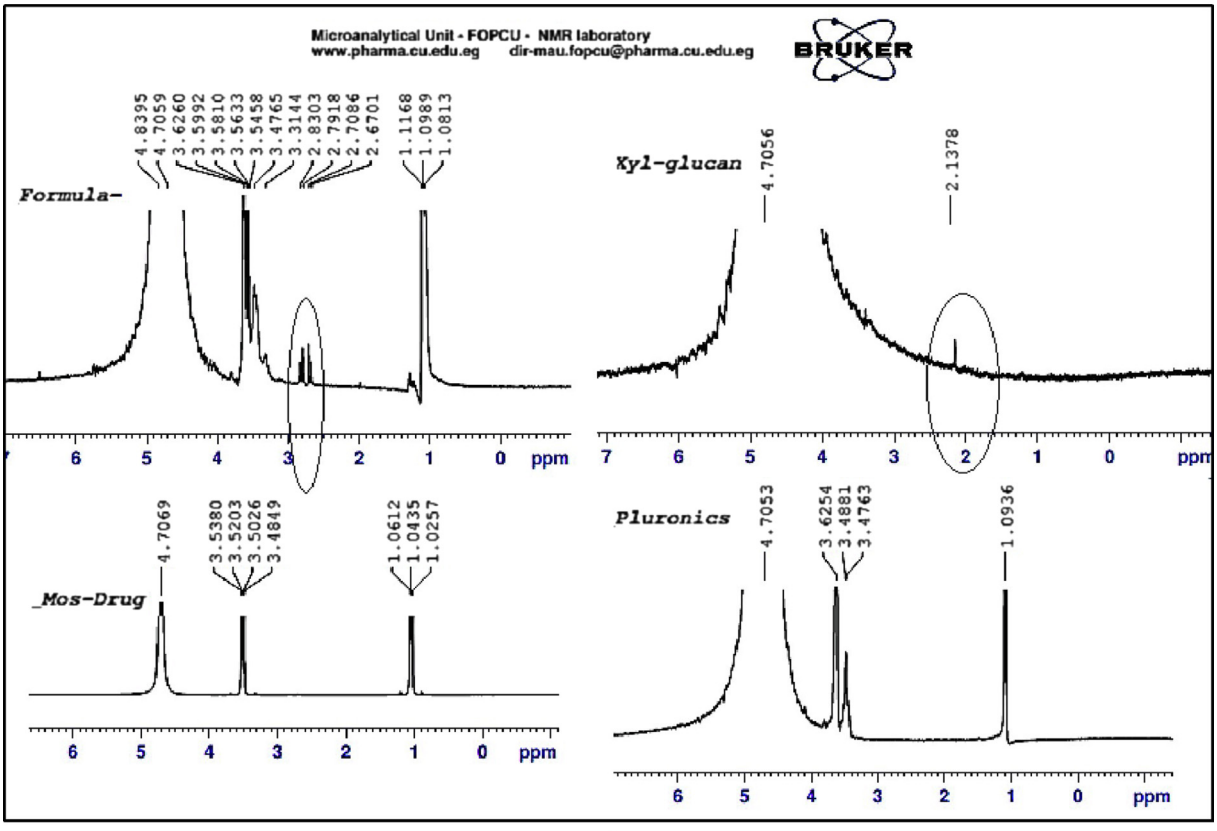

d

Fig. 3 (*continued*)

Table 4
Permeation data parameters.

	r^2	Flux (JSS) ($\mu g/cm^2/min$)	P_{app} (cm^2/min)	ER	D (cm^2/min)	Lag time (T_L) min	% Permeated
MOS-XPM (F4)	0.9941	148.12	0.03	3.36	3.98×10^{-7}	26.43	92.5
Drug Suspension	0.8173	44.07	0.009	–	2.21×10^{-4}	7.54	31.77

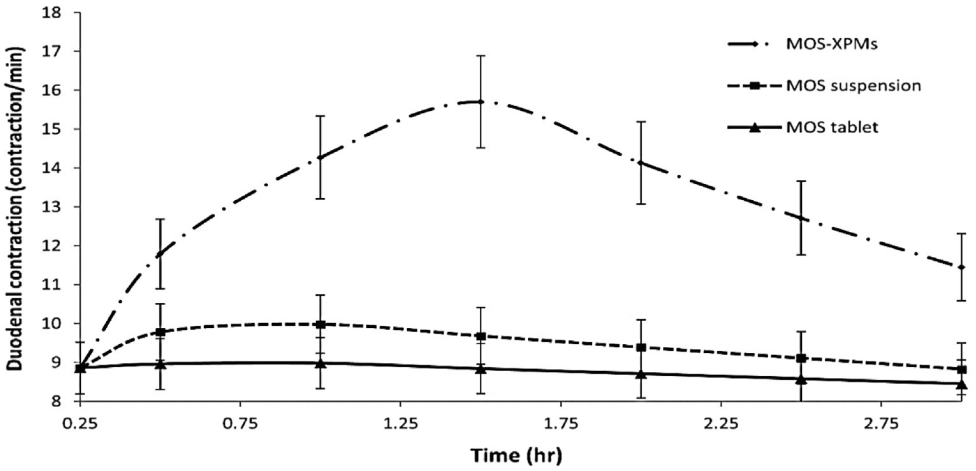

(a)

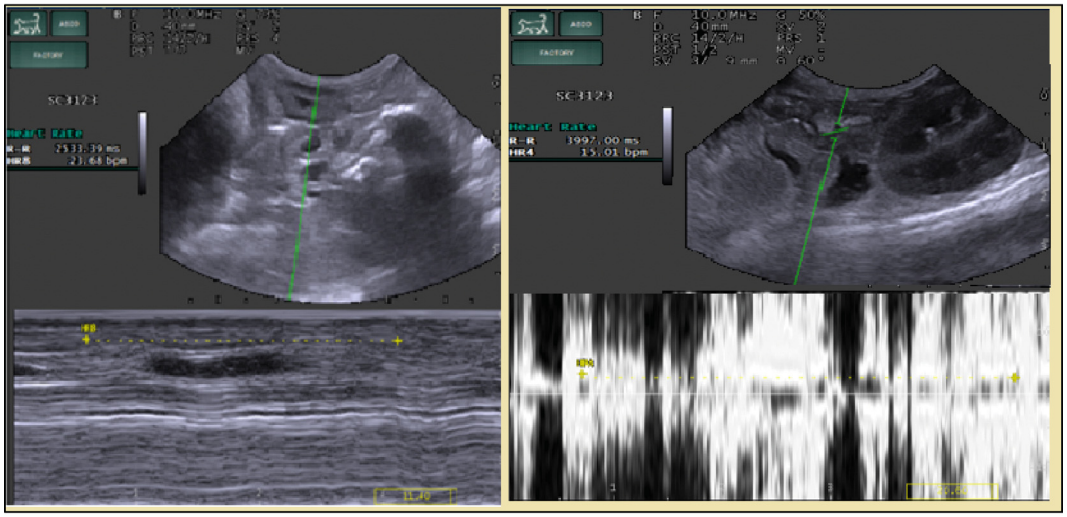

(b)

Fig. 4. (a) Comparative pharmacodynamics studies of commerial MOS oral tablets, MOS suspension and optimized MOS-XPMs ± SD. (b) Ultrasonographic image of the duodenal and cecal contractions after intranasal administration of the prepared mosapride xyloglucan Pluronic micelles (MOS-XPMs), and MOS suspension and oral administration of mosapride® tablet in rabbit.

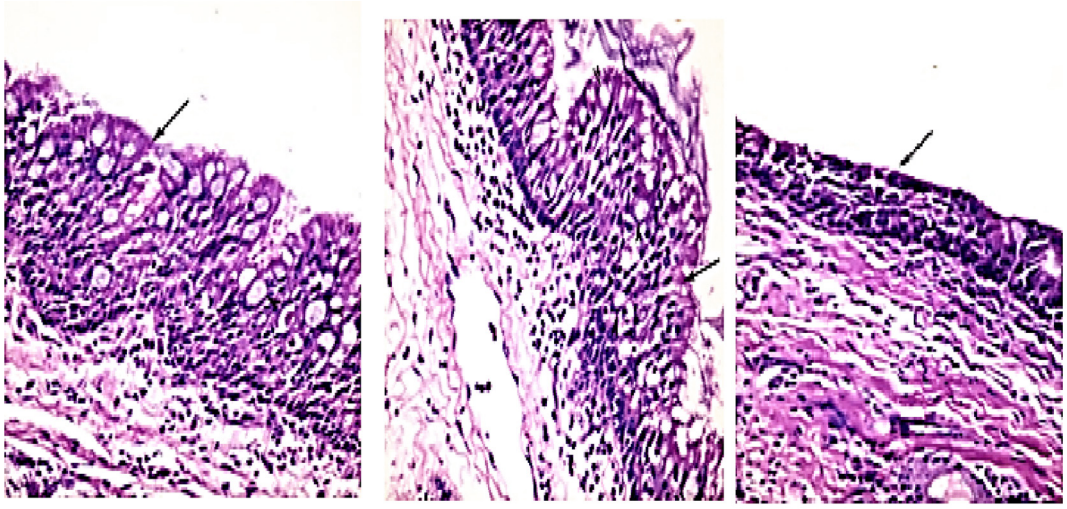

(a) (b) (C)

Fig. 5. Photomicrograph of sheep nasal mucosa of (a) negative control treated with PBS PH6.4) (b) MOS-XPMs showing: pseudo stratified epithelium cell (arrow) and peripheral nerve (N) (H&E) (X: 400) (c) positive control treated with Isopropyl alcohol) showing: degenerative change of pseudo stratified epithelium cell.

control-treated mucosa showed a degenerative change of pseudo-stratified epithelium cells, which ensured the safety of MOS-XPMs in nasal administration.

Conclusion

The MOS-XPMs was successfully prepared with PP123:PF127 ratio of 30:70, drug-to-Pluronic ratio of 1:2, and xyloglucan concentration (1% wt.). Xyloglucan cross-linked in the polymeric micelle shell and conferred higher stability to the prepared MOS-XPMs and higher contact time with nasal mucosa. The MOS-XPMs improved significantly the nasal permeation and the duodenal and cecal contractions through direct systemic absorption, which ensured higher bioavailability than MOS suspension and oral marketed tablets. Thus, the intranasal MOS-XPMs could be a novel delivery system and a promising alternative to the oral delivery of mosapride.

Declaration of Competing Interest

The authors declare that they have no known competing financial interests or personal relationships that could have appeared to influence the work reported in this paper.

Acknowledgement

The ultrasonographic examination was conducted with the help of Dr. Mohamed Elsaid Associate Lecturer, Faculty of Veterinary Medicine, Cairo University. Authors want to thanks Dr. Ethar Abdel Raouf for her kind assistance.

Appendix A. Supplementary material

Supplementary data to this article can be found online at https://doi.org/10.1016/j.jare.2020.01.013.

References

[1] Quigley E. Prokinetics in the management of functional gastrointestinal disorders. J Neurogastroenterol Motil 2015;21:330–6. https://doi.org/10.5056/jnm15094.
[2] Ali AA, Sayed OM. Preparation and characterization of mosapride citrate inclusion complexes with natural and synthetic cyclodextrins. Pharm Dev Technol 2013;18:1–9. https://doi.org/10.3109/10837450.2011.646425.
[3] Sakashita M, Mizuki Y, Yamaguchi T, Miyazaki H, Sekine Y. Pharmacokinetics of the gastrokinetic agent mosapride citrate after intravenous and oral administrations in dogs and monkeys. Arzneimittelforschung 1993;3:864–6. 0004-4172.
[4] Hammad RW, Sanad RAB, Abdelmalk NS, Aziz RL, Torad FA. Intranasal surface-modified mosapride citrate-loaded nanostructured lipid carriers (MOS-SMNLCs) for treatment of reflux diseases: in vitro optimization, pharmacodynamics, and pharmacokinetic studies. AAPS Pharm Sci Tech 2018. https://doi.org/10.1208/s12249-018-1142-9.
[5] ElMeshad AN, El Hagrasy AS. Characterization and optimization of orodispersible mosapride film formulations. AAPS Pharm Sci Tech 2011;12:1384–92. https://doi.org/10.1208/s12249-011-9713-z.
[6] Nour SA, Abdelmalak NS, Naguib MJ, Hassan M, Ibrahim AB. Intranasal brain-targeted clonazepam polymeric micelles for immediate control of status epilepticus : in vitro optimization, ex vivo determination of cytotoxicity, in vivo biodistribution and pharmacodynamics studies Intranasal brain-targeted clonazepam. Drug Deliv 2016:000. https://doi.org/10.1080/10717544.2016.1223216.
[7] Kabanov AV, Alakhov VY. Pluronic? block copolymers in drug delivery: from micellar nanocontainers to biological response modifiers. Crit Rev Ther Drug Carrier Syst 2002;19:1–72. https://doi.org/10.1615/CritRevTherDrugCarrierSyst.v19.i1.10.
[8] Lin HR, Chang PC. Novel Pluronic-chitosan micelle as an ocular delivery system novel pluronic-chitosan micelle as an ocular delivery system. J Biomed Mater Res Part B: Appl Biomater 2012. https://doi.org/10.1002/jbm.b.32871.
[9] Madgulkar A, Bhalekar MR, Dikpati AA. Improving oral bioavailability of acyclovir using nanoparticulates of thiolated xyloglucan. Int J Biol Macromol 2016;89:689–99. https://doi.org/10.1016/j.ijbiomac.2016.02.007.
[10] Mkedder I, Travelet C, Durand-Terrasson A, Halila S, Dubreuil F, Borsali R. Preparation and enzymatic hydrolysis of nanoparticles made from single xyloglucan polysaccharide chain. Carbohydr Polym 2013;94:934–9. https://doi.org/10.1016/j.carbpol.2013.02.001.
[11] Nishinari K, Takahashi R. Interaction in polysaccharide solutions and gels. Curr Opin Coll Interf Sci 2003;8:396–400. https://doi.org/10.1016/S1359-0294(03)00099-2.
[12] Jó TA, Petri DFS, Beltramini LM, Lucyszyn N, Sierakowski MR. Xyloglucan nano-aggregates: physico-chemical characterisation in buffer solution and potential application as a carrier for camptothecin, an anti-cancer drug. Carbohydr Polym 2010;82:355–62. https://doi.org/10.1016/j.carbpol.2010.04.072.
[13] Higuchi Higuchi C. Phase-solubility techniques - Google Scholar. Adv Anal Chem Instrum 1965;4:117–212.
[14] Kumara P, Mohanb C, Uma Shankara MKS, Gulatia M. Physiochemical characterization and release rate studies of solid dispersions of ketoconazole with Pluronic F127 and PVP K-30. Iran J Pharm Res 2011;10:685–94. 17350328.
[15] Liu L, Sun L, Wu Q, Guo W, Li L, Chen Y, et al. Curcumin loaded polymeric micelles inhibit breast tumor growth and spontaneous pulmonary metastasis. Int J Pharm 2013;443:175–82. https://doi.org/10.1016/j.ijpharm.2012.12.032.
[16] Huh KM, Lee SC, Cho YW, Lee J, Jeong JH, Park K. Hydrotropic polymer micelle system for delivery of paclitaxel. J. of Controlled Release 2005;101:59–68. https://doi.org/10.1016/j.jconrel.2004.07.003.
[17] Mahajan HS, Gundare SA. Preparation, characterization and pulmonary pharmacokinetics of xyloglucan microspheres as dry powder inhalation. Carbohydr Polym 2014;102:529–36. https://doi.org/10.1016/j.carbpol.2013.11.036.
[18] Eshel-Green T, Bianco-Peled H. Mucoadhesive acrylated block copolymers micelles for the delivery of hydrophobic drugs. Colloids Surfaces B Biointerfaces 2016;139:42–51. https://doi.org/10.1016/j.colsurfb.2015.11.044.
[19] Abdelbary G, Tadros M. Brain targeting of olanzapine via intranasal delivery of core-shell difunctional block copolymer mixed nanomicellar carriers: In vitro characterization, ex vivo estimation of nasal toxicity and in vivo biodistribution studies. Int J Pharm 2013;452:300–10. https://doi.org/10.1016/j.ijpharm.2013.04.084.
[20] Shah B, Khunt D, Bhatt H, Misra M, Padh H. Intranasal delivery of venlafaxine loaded nanostructured lipid carrier: Risk assessment and QbD based optimization. J Drug Deliv Sci Technol 2016;33:37–50. https://doi.org/10.1016/j.jddst.2016.03.008.
[21] Dina MAA, Omaima AS, Abd EAAE, Demiana IN. Formulation and evaluation of binary and ternary solid dispersions of domperidone by solvent evaporation method. African J Pharm Pharmacol 2014;8:66–80. https://doi.org/10.5897/AJPP2013.1401.
[22] Hussein YHA, Youssry M. Polymeric micelles of biodegradable diblock copolymers: Enhanced encapsulation of hydrophobic drugs. Materials (Basel) 2018;11. https://doi.org/10.3390/ma11050688.
[23] Oh KT, Bronich TK, Kabanov AV. Micellar formulations for drug delivery based on mixtures of hydrophobic and hydrophilic Pluronic® block copolymers. J Control Release 2004;94:411–22. https://doi.org/10.1016/j.jconrel.2003.10.018.
[24] Amann M, Willner L, Stellbrink J, Radulescu A, Richter D. Studying the concentration dependence of the aggregation number of a micellar model system by SANS. Soft Matter 2015;11:4208–17. https://doi.org/10.1039/c5sm00469a.
[25] Vorobyova O, Lau W, Winnik MA. Aggregation number determination in aqueous solutions of a hydrophobically modified poly(ethylene oxide) by fluorescence probe techniques. Langmuir 2001;17:1357–66. https://doi.org/10.1021/la0011026.
[26] Zhao L, Du J, Duan Y, Zang Y, Zhang H, Yang C, et al. Curcumin loaded mixed micelles composed of Pluronic P123 and F68: preparation, optimization and in vitro characterization. Colloids Surfaces B Biointerfaces 2012;97:101–8. https://doi.org/10.1016/j.colsurfb.2012.04.017.
[27] Wei Z, Hao J, Yuan S, Li Y, Juan W, Sha X, et al. Paclitaxel-loaded Pluronic P123/F127 mixed polymeric micelles: Formulation, optimization and in vitro characterization. Int J Pharm 2009;376:176–85. https://doi.org/10.1016/j.ijpharm.2009.04.030.
[28] Suksiriworapong J, Rungvimolsin T, A-gomol A, Junyaprasert VB, Chantasart D. Development and characterization of lyophilized diazepam-loaded polymeric micelles. AAPS PharmSciTech 2014;15:52–64. https://doi.org/10.1208/s12249-013-0032-4.
[29] Mingkwan T, Suksiriworapong J, Chantasart D. Pluronic ® P123/TPGS and pluronic ® F127/TPGS mixed micelles for the entrapment of itraconazole. Chiang Mai J. Sci. 2015;42.
[30] Raval A, Pillai SA, Bahadur A, Bahadur P. Systematic characterization of Pluronic® micelles and their application for solubilization and in vitro release of some hydrophobic anticancer drugs. J Mol Liq 2017;230:473–81. https://doi.org/10.1016/j.molliq.2017.01.065.
[31] Li F, Danquah M, Mahato RI. Synthesis and characterization of amphiphilic lipopolymers for micellar drug delivery. Biomacromolecules 2010;11:2610–20. https://doi.org/10.1021/bm100561v.
[32] Papadopoulou V, Kosmidis K, Vlachou M, Macheras P. On the use of the Weibull function for the discernment of drug release mechanisms. Int. J. Pharm. 2006;309:44–50. https://doi.org/10.1016/j.ijpharm.2005.10.044.
[33] Kosmidis K, Argyrakis P, Macheras P. Fractal kinetics in drug release from finite fractal matrices. J Chem Phys 2003;119:6373–7. https://doi.org/10.1063/1.1603731.
[34] Liu CL, Wu G, Chen SC, You J, Wang YZ. Crystallization induced micellization of poly(p-dioxanone)-block-polyethylene glycol diblock copolymer

functionalized with pyrene moiety. Chinese Chem Lett 2014;25:1311–7. https://doi.org/10.1016/j.cclet.2014.07.009.
[35] Juggernauth KR. Structure-Property Relationships in Clay/Polymer Dispersions : Characterizing Bulk and Nanoscale Changes 2013. http://hdl.handle.net/2027.42/99947.
[36] Sigala PA, Tsuchida MA, Herschlag D. Hydrogen bond dynamics in the active site of photoactive yellow protein. Proc Natl Acad Sci 2009;106:9232–7. https://doi.org/10.1073/pnas.0900168106.
[37] Ghelardi E, Tavanti A, Davini P, Celandroni F, Salvetti S, Parisio E, et al. A mucoadhesive polymer extracted from tamarind seed improves the intraocular penetration and efficacy of rufloxacin in topical treatment of experimental bacterial keratitis. Antimicrob Agents Chemother 2004;48:3396–401. https://doi.org/10.1128/AAC.48.9.3396-3401.2004.
[38] El-Gendy MA, El-Assal MIA, Tadros MI, El-Gazayerly ON. Olmesartan medoxomil-loaded mixed micelles: preparation, characterization and *in-vitro* evaluation. Futur J Pharm Sci 2017:10–4. https://doi.org/10.1016/j.fjps.2017.04.001.
[39] Alai MS, Lin WJ, Pingale SS. Application of polymeric nanoparticles and micelles in insulin oral delivery. J Food Drug Anal 2015;23:351–8. https://doi.org/10.1016/j.jfda.2015.01.007.
[40] Grassin-Delyle S, Buenestado A, Naline E, Faisy C, Blouquit-Laye S, Couderc LJ, et al. Intranasal drug delivery: an efficient and non-invasive route for systemic administration - Focus on opioids. Pharmacol Ther 2012;134:366–79. https://doi.org/10.1016/j.pharmthera.2012.03.003.